Published in final edited form as:
Inorg Chem. 2009 July 6; 48(13): 5758–5771. doi:10.1021/ic802278r.

Cadmium(II) Complex Formation with Cysteine and Penicillamine

Farideh Jalilehvand[*], **Bonnie O. Leung**, and **Vicky Mah**
Department of Chemistry, University of Calgary, Calgary, AB, Canada T2N 1N4

Abstract

The complex formation between cadmium(II) and the ligands cysteine (H_2Cys) or penicillamine (H_2Pen = 3, 3′-dimethylcysteine) in aqueous solutions, containing $C_{Cd(II)} \sim 0.1$ mol dm^{-3} and $C_{H_2L} = 0.2 – 2$ mol dm^{-3}, was studied at pH = 7.5 and 11.0 by means of ^{113}Cd-NMR and Cd K- and L_3-edge X-ray absorption spectroscopy. For all cadmium(II)-cysteine mole ratios the mean Cd-S and Cd-(N/O) bond distances were found in the ranges 2.52 – 2.54 Å and 2.27 – 2.35 Å, respectively. The corresponding cadmium(II)-penicillamine complexes showed slightly shorter Cd-S bonds, 2.50 – 2.53 Å, but with the Cd-(N/O) bond distances in a similar wide range, 2.28 – 2.33 Å. For the mole ratio $C_{H_2L} / C_{Cd(II)} = 2$, the ^{113}Cd chemical shifts, in the range 509 – 527 ppm at both pH values, indicated complexes with distorted tetrahedral $CdS_2N(N/O)$ coordination geometry. With a large excess of cysteine (mole ratios $C_{H_2Cys} / C_{Cd(II)} \geq 10$) complexes with CdS_4 coordination geometry dominate, consistent with the ^{113}Cd NMR chemical shifts, δ ~ 680 ppm at pH 7.5 and 636 - 658 ppm at pH 11.0, and their mean Cd-S distances of 2.53 ± 0.02 Å. At pH 7.5, the complexes are almost exclusively sulfur-coordinated as $[Cd(S\text{-cysteinate})_4]^{n-}$, while at higher pH the deprotonation of the amine groups promotes chelate formation, and at pH 11.0 a minor amount of the $[Cd(Cys)_3]^{4-}$ complex with CdS_3N coordination is formed. For the corresponding penicillamine solutions with mole ratios $C_{H_2Pen} / C_{Cd(II)} \geq 10$, the ^{113}Cd-NMR chemical shifts, δ ~ 600 ppm at pH 7.5 and 578 ppm at pH 11.0, together with the average bond distances Cd-S 2.53 ± 0.02 Å and Cd-O 2.30 – 2.33 Å, indicate that $[Cd(penicillaminate)_3]^{n-}$ complexes with chelating $CdS_3(N/O)$ coordination dominate already at pH 7.5, and become mixed with $CdS_2N(N/O)$ complexes at pH 11.0. The present study reveals differences between cysteine and penicillamine as ligands to the cadmium(II) ion that can explain why cysteine-rich metallothionines are capable of capturing cadmium(II) ions, while penicillamine, clinically useful for treating the toxic effects of mercury(II) and lead(II) exposure, is not efficient against cadmium(II) poisoning.

Keywords

Cadmium(II); cysteine; penicillamine; EXAFS; Cd L_3-edge XANES; ^{113}Cd NMR; solution

Introduction

Cadmium(II) is generally known as a non-essential, highly toxic metal ion that acts as a carcinogen in mammals, inhibits growth of plants by interfering with photosynthesis and nitrogen metabolism, and decreases uptake of water and minerals [1]. Recent studies, however, on the marine diatom *Thalassiosira weissflogii* showed evidence of the first cadmium specific enzyme, cadmium(II)-carbonic anhydrase, which actually has a preliminary function in the diatom's photosynthesis by catalyzing the dehydration of HCO_3^- to CO_2 [2,3].

[*]Author to whom correspondence should be addressed. Email: faridehj@ucalgary.ca.

Supporting Information **Available.** Diagrams for the distribution of cadmium(II) cysteine and penicillamine complexes, EXAFS curve-fitting results for CdS_3O and CdS_2N_2 model compounds, comparison of the EXAFS spectra for solutions **E** – **G, H** and **L** (pH 7.5 and 11), and **L2** - **N2**. This material is available free of charge via the Internet at http://pubs.acs.org.

A well-known example of cadmium poisoning is the *Itai-Itai* disease (*Itai* = pain in Japanese), which was caused by cadmium released from mining waste into the Jinzu river in Japan, contaminating large agricultural areas [4]. Metallothioneins (MTs), which are a family of cysteine-rich polypeptides with low molecular weight [5], are active *in vivo* in removing heavy metal ions such as Cd^{2+} and Hg^{2+} through thiolate coordination from the cysteine residues [6-8]. Even though the toxic effects of cadmium(II) are inhibited when bound to metallothionein (Cd-MT), a sufficient amount of MT must be synthesized *in vivo* to block cadmium toxicity [5]. Cadmium(II) mainly accumulates in the liver (80-90% as Cd-MT) and to a lesser extent in the kidneys (55-65% as Cd-MT) and other tissues [9].

No effective antidote is known to counteract cadmium poisoning, although to some extent cysteine (H_2Cys), homocysteine, *N*-acetylcysteine and glutathione prevent cell uptake by binding to cadmium(II) through their thiol groups [5,10]. On the other hand penicillamine (3,3′-dimethylcysteine), commonly used in reducing toxic effects of mercury and lead exposure, is not efficient in cadmium(II) treatments [11]. We have studied the structure and coordination of the cadmium(II) complexes formed with cysteine and penicillamine both at pH 7.5 and 11.0 in aqueous solutions containing $C_{Cd(II)} \sim 0.1$ mol dm^{-3} for ligand to metal ratios from 2.0 to 20, to find explanations for the different efficiencies that would allow for more effective detoxifying chelating agents to be designed.

There are numerous reports on formation constants of cadmium(II) cysteine complexes; however, differences in the experimental conditions (e.g. temperature, ionic medium, concentration range) restrict their applicability for the present investigation [12,13]. We have used the formation constants determined through potentiometric methods by Cole *et al.* [14] to generate the diagrams showing the distribution of the complexes vs. pH that are displayed in Figure S-1.

In a similar study, Corrie and coworkers reported mononuclear cadmium(II)-penicillamine complex formation in 3 mol·dm^{-3} $NaClO_4$ as ionic medium [15]. Avdeef and Kearney interpreted alkalimetric titrations of cadmium(II)-penicillamine solutions with protonated polynuclear complexes dominating in the pH range 4 – 8 [16] and suggested that the formation of these complexes was suppressed at high ionic strength. The formation constants from both studies have been used to generate the distribution diagrams shown in Figures S-2a and S-2b.

In the current study, we have combined ^{113}Cd NMR and X-ray absorption spectroscopy (Cd K-edge EXAFS and Cd L_3-edge XANES) to investigate the structure of cadmium(II) complexes with cysteine or penicillamine as ligands in aqueous solution. Recent development has made ^{113}Cd NMR a useful technique for classifying the coordination environment in cadmium(II) complexes. The ^{113}Cd NMR chemical shift shows a strong correlation to the type of coordinating ligand atom, with sulfur as the most deshielding, followed by nitrogen and finally oxygen [17,18]. Chemical shifts reported for several biologically relevant mononuclear cadmium(II) thiolate complexes are collected in Table 1, including solid state δ_{iso} (^{113}Cd) for cadmium(II) cysteaminate complex with CdS_3N_2 coordination geometry for comparison. It should be emphasized, however, that ^{113}Cd NMR chemical shifts cannot only be interpreted based on the type and number of donor atoms (e.g. S, N or O), since cadmium magnetic shielding tensors are sensitive to many other factors such as the type of the ligand, its coordination mode (bridging vs. terminal) and coordination number/geometry of cadmium(II) ions (i.e. 4-, 5- or 6-coordinated) [19].

For CdS_4 coordination the observed $\delta(^{113}Cd)$ range is rather wide. High frequency $\delta(^{113}Cd)$ shifts have been reported for $[Cd(S\text{-cysteinate})_4]^{2-}$ in cadmium(II)-substituted LADH (751 ppm) [20], rubredoxin (723 - 732 ppm) [21,22], and the DNA binding domain of the glucocorticoid hormone receptor (704, 710 ppm) [23]. For a designed cysteine-rich TRI peptide

bound to cadmium(II) two signals were observed at 650 and 680 ppm for the distorted tetrahedral CdS_4 sites, with the difference originating from "small geometric orientations in the coordination environment" [24]. For CdS_4 sites with bridging thiolate groups, the chemical shifts are generally more shielded. Examples are the dinuclear cadmium(II) binding site of the GAL4 protein (669 and 707 ppm) [25,26], and Cd(II)-loaded metallothionine (Cd_7-MT) with several resonances in the 610 – 680 ppm region, which were interpreted as evidence for two sets of clusters, Cd_3S_9 and Cd_4S_{11}, with bridging cysteine sulfur atoms [17].

Pecoraro *et al.* recently reported ^{113}Cd NMR chemical shifts for the first water-soluble three-coordinated CdS_3 structure (δ = 684 - 690 ppm), using designed peptides that specifically bind cadmium(II) ions via bulky Pen residues [27-29]. The result calls for re-evaluation of an earlier assignment of the ^{113}Cd chemical shift 572 ppm to a pure CdS_3 coordination [30].

The X-ray absorption near edge structure (XANES) region of the cadmium L_3-edge has been proposed to be sensitive to the local structure around cadmium, and displays a characteristic pre-edge peak for cadmium complexes with oxygen or nitrogen coordination, while for tetrahedral CdS_4 coordination the edge is smooth and almost featureless [31,32]. We recently measured the Cd L_3-edge XANES spectra for a series of crystalline cadmium complexes with $CdS_x(N/O)_y$ configurations and observed that the distinct pre-edge peak at 3539.1 eV (corresponding to a Cd 2p → 5d transition) in the $Cd(ClO_4)_2{\cdot}6H_2O$ spectrum (CdO_6 model) gradually merges into the absorption edge of the model compounds for CdS_2O_4, CdS_3O_3, CdS_6, CdS_3O and CdS_2N_2 coordination, and finally disappears in the CdS_3N_2 and CdS_4 spectra [33].

The present study on cadmium(II) complex formation with cysteine and penicillamine is part of a continuing project to obtain structural information on complexes of heavy metals with biomolecules to facilitate understanding of the function of such species in biological systems [34].

Experimental Section

Sample preparation

Cadmium(II) perchlorate hydrate $Cd(ClO_4)_2{\cdot}6H_2O$, L-cysteine, D-penicillamine and sodium hydroxide (Sigma Aldrich) were used without further purification. The preparations were performed under argon atmosphere using oxygen-free boiled water to prevent oxidation of the cysteine and penicillamine ligands. The pH of the solutions was monitored with a Corning Semi-Micro electrode.

Cadmium(II) cysteine/ penicillamine solutions

Table 2 presents the compositions of the cadmium(II)-cysteine (**A** – **G**) and the cadmium(II)-penicillamine (**H** – **N**) solutions, which were prepared with ligand / metal mole ratios C_{H_2L} / $C_{Cd(II)}$ from 2.0 to 20, and adjusted to different pH values (7.5 and 11.0) in two series. Cysteine or penicillamine (2 – 20 mmol) was dissolved in oxygen-free water (containing 10% D_2O) and a weighed amount of $Cd(ClO_4)_2{\cdot}6H_2O$ (1 mmol) was added. A white precipitate immediately formed with cysteine and the pH ~1.6 was recorded; no precipitate was formed for penicillamine. Dropwise addition of 6 mol·dm^{-3} NaOH dissolved the precipitate around pH ~ 6 – 7 (the lower pH for high L / M ratios), and the clear solutions were collected at pH 7.5 and 11.0. The total cadmium(II) concentration was checked for **A2** – **E2** and **H2** – **L2** with a Thermo Jarrell Ash AtomScan 16 inductively coupled plasma atomic emission spectrophotometer (ICP-AES).

^{113}Cd NMR measurements

The ^{113}Cd NMR spectra shown in Figures 1 and 2 were collected at 300 K (27 °C) with a Bruker AMX2-300 spectrometer at 66.6 MHz, using a 10 mm broadband (BBO) probe, a 7.0 microsecond 90° pulse and recycle delay of 5.0 seconds. All solutions contained ~ 10% D_2O. A 0.1 mol·dm^{-3} solution of $Cd(ClO_4)_2{\cdot}6H_2O$ in D_2O was used as external reference (0 ppm) [18]. All spectra were proton decoupled and measured with a sweep width of 850 – 900 ppm. The total number of collected scans for the cadmium(II) cysteine and penicillamine solutions, as well as the FWHH of the NMR signals, are shown in Table S-1.

X-ray absorption spectroscopy

Cadmium K-edge extended X-ray absorption fine structure (EXAFS) spectra were collected at BL 2-3 and 7-3 at the Stanford Synchrotron Radiation Lightsource (SSRL) under dedicated conditions of 3.0 GeV and 70-100 mA. Higher harmonics from a Si[220] double crystal monochromator were rejected by detuning to 50% of the maximum incident beam intensity. The spectra were recorded in transmission mode, with argon in the first ion chamber (I_0) and krypton in the second (I_1) and third (I_2) ion chambers. The solutions were enclosed in 10 mm Teflon spacers between 4 μm polypropylene film windows. Three to five scans were collected for each sample. Before averaging, the energy scale was externally calibrated for each scan by assigning the first inflection point of the Cd K-edge of a Cd foil to 26711.0 eV.

The Cd L_3-edge XANES measurements were performed at beamline 9-A of the High Energy Accelerator Research Organization (Photon Factory), Tsukuba, Japan. The ring operates under dedicated conditions at 2.5 GeV and 350 – 400 mA. The data were collected in fluorescence mode with helium in the first ion chamber (I_0) and an argon-filled Lytle detector (I_f). Higher harmonics from a Si[111] double crystal monochromator were rejected by means of nickel and rhodium coated mirrors. Solution samples were enclosed in 5 mm Teflon spacers between 4 μm polypropylene windows. For each sample 2-3 scans were collected, externally calibrated by assigning the first inflection point of the Cd L_3-edge of a Cd foil to 3537.6 eV, and then averaged.

XAS data analysis

The WinXAS 3.1 program suite was used for the data analysis [35]. The background absorption was subtracted with a first-order polynomial over the pre-edge region, followed by normalization of the edge step. For the Cd K-edge XAS spectra, the energy scale was converted into *k*-space, where $k = (8\pi^2 m_e/h^2)(E-E_0)$, using the threshold energy E_0 = 26710.0 – 26711.3 eV. The EXAFS oscillation was then extracted using a 7-segment cubic spline to remove the atomic background absorption above the edge.

The EXAFS model functions, $\chi(k)$, were constructed by means of the FEFF 8.1 program [36, 37], to obtain *ab initio* calculated amplitude $f_{eff}(k)_i$, phase shift $\varphi_{ij}(k)$, and mean free path $\lambda(k)$ functions (eq. 1). The FEFF input file was generated by means of the ATOMS program [38], using structural information from the crystal structure of the reference compound Cd$(SCH_2CH_2NH_2)_2$ (as CdS_3N_2 model) with both short and long Cd-S, Cd-N(/O) and Cd-Cd distances [39]. Note that two neighboring elements in the periodic table (such as oxygen and nitrogen) obtain very similar amplitude functions $f_{eff}(k)_i$ and cannot be distinguished by EXAFS.

$$\chi(k) = \sum_i \frac{N_i \cdot S_0^2(k)}{k \cdot R_i^2} |f_{eff}(k)|_i \cdot \exp(-2k^2\sigma_i^2) \cdot \exp[-2R_i/\lambda(k)] \cdot \sin\left[2kR_i + \varphi_{ij}(k)\right] \quad (1)$$

The structural parameters were refined by least-squares methods, fitting the k^3-weighted model function $\chi(k)$ to the experimental unfiltered EXAFS oscillation generally over the k range 3.5 – 12.0 Å $^{-1}$ (11.2 Å $^{-1}$ for the solution **A2**), allowing the bond distance (R), Debye-Waller parameter (σ) and ΔE_0 (correlated parameter for all scattering paths) to float, while the amplitude reduction factor (S_0^2) and / or coordination number (N) were fixed. The fitting results are shown in Figures 3, 4, Tables 3 and 4. The estimated errors of the refined coordination numbers, bond distances and their Debye-Waller parameters for the dominating Cd-S path are estimated to be within 20%, ± 0.02 Å and ± 0.001 Å^2, respectively, including effects of systematic deviations. The corresponding structural parameters for the Cd-(N/O) path are less accurate, i.e. ± 0.04 Å and ± 0.003 – 0.005 Å^2 for bond distances and Debye-Waller parameters, respectively, due to the difficulties associated with separating the EXAFS contribution from the light oxygen and nitrogen atoms from that of the heavier sulfur atom.

Results

^{113}Cd NMR spectroscopy

The ^{113}Cd-NMR spectra obtained for the cadmium(II)-cysteine solutions containing $C_{Cd(II)}$ ~ 0.1 mol·dm^{-3} at pH 7.5 (**A1 – G1**) and 11.0 (**A2 – G2**) are shown in Figure 1. The solutions contain several cadmium(II) cysteine species, as indicated by the distributions of complexes calculated for compositions corresponding to solutions **A**, **B**, **D** and **E**, with the use of the equilibrium constants in Ref. 14; see Figure S-1. The increase in the total cysteine concentration in solutions **B – G**, resulted in more deshielded ^{113}Cd chemical shifts, indicating a high degree of thiol coordination in the cadmium(II) complexes [17]. For solutions **A** - **C**, chemical exchange reactions with intermediate rate (on the NMR time scale) between the several Cd (II)-species in equilibrium resulted in an averaged broad signal for each solution. Considerably sharper NMR signals were obtained for solutions **D** - **G** with high total cysteine concentration, which may be due to a single dominating cadmium(II) complex, and/or faster ligand exchange between different cadmium(II) species in the solution. The alkaline solutions **B2** - **G2** showed somewhat more shielded chemical shifts than the corresponding solutions **B1** - **G1** at pH = 7.5, probably due to an increase in chelate Cd(II)-(*S*,*N*-Cys) coordination of the cysteinate ligands (Cys^{2-}) when the amine group deprotonates at higher pH. The NMR signals were generally narrower for alkaline solutions than for the corresponding neutral ones, especially for **A2** - **C2**, which indicates a faster ligand exchange process, probably promoted by the increasing availability of -NH_2 groups or OH^- ions.

The ^{113}Cd NMR spectra for the cadmium(II)-penicillamine solutions (**H** – **N**) with C_{H_2Pen} / $C_{Cd(II)}$ ratios from 2 to 20 are shown in Figure 2, and the distributions of the cadmium(II)-penicillamine complexes for solutions **H**, **I**, **K** and **L** according to the available stability constants [15] are presented in Figure S-2. The observed chemical shifts for solutions **H1** and **H2** containing C_{H_2Pen} = 0.2 mol·dm^{-3} were close to those of the corresponding cadmium(II) cysteine solutions **A1** and **A2**, and therefore similar coordination environments are expected around the cadmium(II) ions.

As for the cadmium(II)-cysteine solutions, the increase in total concentration of penicillamine for solutions **H** to **N**, resulted in more deshielded NMR signals, even though the range of $\Delta\delta$ (^{113}Cd) was considerably more limited. At pH 7.5 the NMR peak for cadmium(II)-penicillamine solutions shifts from 509 ppm to 607 ppm for **H1** to **M1** (~ 100 ppm), while for the corresponding cysteine solutions the shift is from 518 ppm to 679 ppm (~ 160 ppm) for **A1** to **F1**. A similar decrease was observed for the alkaline solutions, with the difference ~ 70 ppm between the ^{113}Cd chemical shifts for the Cd(II)-penicillamine solutions **H2** and **N2**, at 510 and 578 ppm, respectively, compared with the difference ~ 130 ppm between the Cd(II)-cysteine solutions **A2** and **G2** at 527 and 658 ppm, respectively. This indicates a higher

tendency for Cd(II) ions to coordinate to the thiolate groups from cysteine than from penicillamine.

The NMR peaks for all the alkaline cadmium(II)-penicillamine solutions (**H2** - **N2**) were sharp, while at pH 7.5 the peaks were broader, especially for solutions **H1** - **K1**, indicating ligand exchange with intermediate rate (on the NMR time scale) between cadmium(II) penicillamine complexes. For solution **H1** (H_2Pen / Cd(II) = 2.0, pH = 7.5), the broad ^{113}Cd resonance became much sharper as the solution pH is increased to 11.0 in **H2**, while remaining in the same position at 510 ppm. This signal is even sharper than that of the corresponding cadmium(II)-cysteine solution **A2**, indicating that a single stable cadmium(II) complex with penicillamine is formed in **H2,** probably $[Cd(Pen)_2]^{2-}$ according to the calculated distribution diagram in Figure S-2.

X-ray absorption spectroscopy - Cd K-edge EXAFS

The least squares curve-fitting results for the k^3-weighted Cd K-edge EXAFS spectra of the cadmium(II) cysteine and penicillamine solutions are shown in Tables 3 and 4, Figures 3 and 4. Since coordination number, amplitude reduction factor (S_0^2) and Debye-Waller parameters (σ^2), all contribute to the amplitude of the EXAFS oscillation and are strongly correlated, the S_0^2 value was kept constant at 0.87 in all refinements to facilitate comparisons. This value was chosen by calibrating the amplitude reduction factors to 0.87 and 0.85 for two crystalline cadmium(II) complexes, imidazolium tris(thiosaccharinato)aqua cadmate(II) (HIm)[Cd(tsac)$_3$(H_2O)] (CdS_3O model) and bis(thiosaccharinato)bis(imidazole) cadmium(II) [Cd(tsac)$_2$(Im)$_2$] (CdS_2N_2 model), respectively; see Figures S-3a and S-3b [40]. The estimated error in the coordination numbers obtained in the refinement procedure is ~ 20%. For each solution two fitting models were applied: one with only a single Cd-S shell, and the other including both Cd-S and Cd-(N/O) scattering paths. Often the fitting residuals had very minor differences, and only by combining with information from the ^{113}Cd NMR chemical shifts, the more appropriate model could be chosen. For most cadmium(II)-cysteine and penicillamine solutions, the mean Cd-S and Cd-(N/O) bond distances were obtained within the ranges 2.52 – 2.54 Å and 2.28 – 2.35 Å, respectively, which are consistent with what is expected for cadmium(II) complexes with tetrahedral $CdS_2(N/O)_2$, $CdS_3(N/O)$ and CdS_4 configuration [*Supporting Material in* Ref. 33]. However, the contribution from the light coordinated atoms (oxygen or nitrogen) to the EXAFS oscillation is difficult to separate from the dominating backscattering of the sulfur atoms, and therefore, in the model refinements the coordination number for the Cd-(N/O) scattering pathway often was fixed at N = 1 or 2, based on the observed ^{113}Cd chemical shift values.

X-ray absorption spectroscopy - Cd L_3-edge XANES

The normalized Cd L_3-edge XANES spectra and the corresponding smoothed 2nd derivatives for the cadmium(II)-cysteine solutions **A2** – **G2** (pH 11.0), as well as those of a few related crystalline compounds with $CdS_x(N/O)_y$ coordination, are shown in Figure 5. The XANES spectra of solutions **A2** – **G2** were rather similar with only a gradual change in the second derivatives. For solutions **A2** – **D2** the XANES spectra and their 2nd derivatives were intermediate to the spectra of Cd(cysteaminate)$_2$ (as CdS_3N_2 model) and bis(thiosaccharinato) bis(imidazole) cadmium(II) [Cd(tsac)$_2$(Im)$_2$] (as CdS_2N_2 model) (Figures 5 and S-4) [39,40]. As the amount of cysteine in solutions **E2** – **G2** increased to a 10 – 20 fold excess of the ligand, the relative intensity of the two main features in the 2nd derivative gradually became almost equal. For solution **G2** both the Cd L_3-edge XANES spectrum and its 2nd derivative are quite similar to those for the CdS_4 standard complex, $(Et_3NH)_4[S_4Cd_{10}(SPh)_{16}]$ (Figures 5 and S-4).

For the cadmium(II) penicillamine solutions **H2** – **N2**, the Cd L_3-edge XANES spectra and corresponding smoothed 2nd derivatives appeared quite similar, as expected from the small difference, 68 ppm, between the ^{113}Cd NMR chemical shifts of solutions **H2** and **N2,** and no

further structural information was gained from the comparison with L_3-edge spectra of standard models (Figure 5).

Discussion

Cadmium(II) Cysteine Solutions

Solution **A1** containing C_{H_2Cys} = 0.2 mol·dm^{-3} was obtained by dissolving the $Cd(HCys)_2$ precipitate by adding NaOH. While the ^{113}Cd NMR spectrum of the solid $[Cd(HCys)_2]\cdot H_2O$ compound showed a broad signal with peak maximum at ~640 ppm [33], in solution the resonance shifts to 518 ppm (pH = 7.5), and then to 527 ppm at pH = 11.0 (**A2**). We recently proposed an oligomeric, "cyclic / cage" type of structure for the solid $[Cd(HCys)_2]\cdot H_2O$ compound with the cadmium(II) ions in CdS_3O and / or CdS_4 coordination sites, similar to **a** in Scheme 1 [33]. When it dissolves in solution **A1**, several species may exist in equilibrium (Scheme 1, b – e), including $[Cd(HCys)(Cys)]^-$ and $[Cd(Cys)_2]^{2-}$ complexes, as indicated in the reported formation constants (Figure S-1, *top left*) [14]. However, any appreciable amount of an oligomeric complex similar to **a** does not seem likely in solution, because of the shift of the ^{113}Cd-NMR signal from ~ 640 ppm for the $[Cd(HCys)_2]\cdot H_2O$ compound to a more shielded region (~ 520 ppm) for solution **A1**, which corresponds to two sulfur atoms in the coordination sphere of cadmium(II) ion. Neither is complex **b** with CdS_2O_2 coordination likely to be present. The only reported CdS_2O_2 complexes, cadmium(II) thio-β-diketonate in acetone, 191 ppm [41], and two bis(phenoxide) bis(tetrahydrothiphene) cadmium(II) complexes, 76 and 144 ppm [42], show considerably higher shielding than that of solution **A1** (518 ppm). However, these complexes contain S-donor ligands other than thiolates and as discussed elsewhere [33], for a cadmium(II) thiolate complex with a stable CdS_2O_2 coordination environment, a ^{113}Cd chemical shift of ~ 400 ppm would be expected.

The coordination site for **d** is similar to that of cadmium(II)-substituted horse liver alcohol dehydrogenase (LADH), with the ^{113}Cd chemical shift 483 ppm for CdS_2NO_{water} coordination [20]. In a large excess of imidazole, the ^{113}Cd chemical shift for Cd(II)-LADH was observed at 519 ppm, which has been assigned to CdS_2N_2 coordination (see Table 1), similar to the coordination site of **e** in Scheme 1. Based on recent theoretical calculations of ^{113}Cd chemical shifts for proteins and model systems, it was proposed that the contribution for each type of ligand in a "tetrahedral" coordination geometry is: δ_S = 187 ppm, δ_N = 77 ppm, $\delta_O(COO^-)$ = -25 ppm and $\delta_O(H_2O)$ = -53 ppm [43], i.e., the carboxylate oxygen is somewhat less shielding than water. Therefore, the ^{113}Cd chemical shift for complex **c** is expected to be more deshielded than that of complex **d**, i.e. ~ 500 ppm.

Hence, the broad peak observed at 518 ppm in the ^{113}Cd NMR spectrum of solution **A1** (pH = 7.5) is proposed to result from a ligand exchange with intermediate rate (on the NMR time scale) between species **c**, **d** and **e** with $CdS_2N(N/O)$ coordination, with estimated ^{113}Cd chemical shifts of ~ 500 ppm ($CdS_2NO_{COO^-}$), ~ 480 ppm (CdS_2NO_{water}) and ~ 520 ppm (CdS_2N_2), respectively. When raising the pH to 11.0 (solution **A2**) the ^{113}Cd NMR signal shifts slightly downfield to 527 ppm, probably due to the complete deprotonation of the amine group, which allows the $[Cd(Cys)_2]^{2-}$ chelate complex (**e**) with CdS_2N_2 coordination to dominate in the solution (Scheme 2).

Least-squares curve-fitting of the Cd K-edge EXAFS spectrum of **A1** shows the minimum residual for a single Cd-S shell model with refined coordination number of ~ 3.6 (Table 3). However, such a high number of sulfur backscatters should correspond to a $\delta(^{113}Cd)$ value of at least 600 ppm (see Table 1), and also is not consistent with the stoichiometric ratio of H_2Cys / Cd(II) = 2.0 in solution **A1**. Although the fitted two-shell model shows slightly higher residuals, the differences between the fits are insignificant. The model including two Cd-(N/O) resulted in a coordination number of 1.9 for the Cd-S path. The Cd-S and Cd-(N/O) bond

distances were 2.54 ± 0.02 and 2.34 ± 0.04 Å, respectively, which fits well with a mixture of $[Cd(HCys)(Cys)]^-$ (CdS_2NO) and $[Cd(S,N\text{-}Cys)_2]^{2-}$ (CdS_2N_2) species (**c** - **e**, Scheme 1) with distorted tetrahedral geometries.

EXAFS curve-fitting for solution **A2** using the same $CdS_2(N/O)_2$ model results in a similar mean Cd-S distance, 2.53 ± 0.02 Å, while the average Cd-(N/O) distance, 2.29 ± 0.04 Å, is slightly shorter than that of solution **A1**. This is consistent with an increase of the dominating $[Cd(S,N\text{-}Cys)_2]^{2-}$ (CdS_2N_2) chelate complex (Scheme 1 e) with stronger bonds between the cadmium(II) ions and the deprotonated cysteine amine groups ($-NH_2$), and the observed ^{113}Cd NMR chemical shift at 527 ppm. For ten structurally known cadmium(II) complexes with CdS_2N_2 configuration, the average Cd-S and Cd-N distances are 2.473 and 2.288 Å, respectively [*Supporting Material in* Ref. 33], with the former slightly shorter than that of solution **A2**. Figure 6 presents the separate contributions to the fitted EXAFS model for solution **A2**.

For solutions **F1** and **G1** with large cysteine excess (C_{H_2Cys} ~ 1.5 mol dm^{-3}), probably with partially protonated amino groups ($HCys^-$) at pH = 7.5, the ^{113}Cd chemical shift is ~ 680 ppm, close to that of solution **E1** (677 ppm). These chemical shifts are higher than the $\delta(^{113}Cd)$ ranges for CdS_3O and CdS_3N, but rather similar to those recently reported for CdS_3 configurations (Table 1). However, the mean Cd-S bond distances, 2.52 - 2.53 Å, obtained from EXAFS spectra of these solutions (Table 3) are much longer than the average Cd-S bond distance in three crystalline CdS3 thiolate complexes (2.446 Å; *Supporting Material in* Ref. 33). For cadmium(II)-substituted rubredoxin from *Clostridium pasteurianum*, a crystal structure determination at 1.5 Å resolution resulted in an average Cd-S distance of **~** 2.5 Å for a CdS4 center [44]. For $[Cd(S\text{-cysteinate})_4]^{2-}$ complexes, there are several reports of higher frequency $\delta(^{113}Cd)$ shifts, e.g. for cadmium(II)-substituted LADH (751 ppm) [20], rubredoxin (723 - 732 ppm) [21,22], and the DNA binding domain of the glucocorticoid hormone receptor (704, 710 ppm) [23]. However, recently the chemical shifts from a designed cysteine-rich TRI peptide at $\delta(^{113}Cd)$ = 650, 680 ppm could, with support from perturbed angular correlation (PAC) spectroscopy, be attributed to distorted tetrahedral $[Cd(S\text{-cysteinate})_4]^{2-}$ complexes [24]. Therefore, based on the ^{113}Cd NMR chemical shift, solutions **E1** - **G1** may contain 100% $[Cd(S\text{-cysteinate})_4]^{n-}$ (with the cysteine ligands in $HCys^-$ or Cys^{2-} forms), or a combination of CdS_4 and $CdS_3(N/O)$ species.

The EXAFS spectra of solutions **E1** – **G1** overlap (see Figure S-5), as expected from the similarity of their ^{113}Cd chemical shifts (677 – 680 ppm). Least-squares curve-fittings of these EXAFS spectra using only a single Cd-S shell resulted in a refined coordination number of 3.8 - 4.1. When the Cd-(N/O) path with a fixed contribution N = 1 is included in the fitting model, the frequency/ coordination number for the Cd-S path refined to N ~ 3 for solutions **E1** and **G1**. Both models yielded similar residuals and reasonable distances (except **F1**), but too low / high Debye-Waller parameters for Cd-(N/O) path. Therefore, the information from Cd K-edge EXAFS data analyses for solutions **E1** - **G1** does not confirm whether or not these solutions contain CdS_4 species exclusively.

The k^3-weighted EXAFS oscillations of the corresponding alkaline (pH = 11.0) solutions **F2** – **G2** containing deprotonated Cys^{2-} virtually overlap (see Figure S-6). However, their increasing ^{113}Cd chemical shifts, 636 ppm (**E2**), 654 ppm (**F2**) and 658 ppm (**G2**), are more sensitive to small changes in the distribution of the complexes than the mean Cd-S bond distances from EXAFS spectroscopy (Table 3). The ^{113}Cd chemical shifts for **F2** and **G2** are in between the values reported for CdS_3N configuration (see Table 1) and the distorted $[Cd(S\text{-cysteinate})_4]^{2-}$ complexes in the TRI peptide. The Cd K-edge EXAFS model fittings for these solutions resulted in very similar residuals for the CdS_4 or CdS_3N models (Table 3). However, the features in the Cd L_3-edge XANES spectra of **F2** and **G2**, and their corresponding

2nd derivatives, are almost identical to those of the CdS_4 model compound (see Cd L_3-edge XANES section above). Therefore, with emphasis on the Cd L_3-edge XANES spectra, we propose that at pH = 11 the dominating complex is $[Cd(S\text{-}Cys)_4]^{6-}$ with fully deprotonated Cys^{2-} ligands in the cadmium(II) cysteine solutions with $C_{H_2Cys} > 1.0$ mol dm^{-3} (**F2** – **G2**; δ (^{113}Cd) = 654 – 658 ppm), together with a minor amount of the $[Cd(Cys)_3]^{4-}$ (CdS_3N) complex. Those species (**h** and **j** in Scheme 2) are in equilibrium with fast ligand-exchange, which results in one averaged signal in their NMR spectra. In the corresponding solutions at pH = 7.5 (**E1** – **G1**), with ^{113}Cd NMR signals at 677 – 680 ppm and partially protonated amine groups, $[Cd(S\text{-cysteinate})_4]^{n-}$ (CdS_4) species are predominantly formed.

In the solution **E2**, the $[Cd(Cys)_3]^{4-}$ (CdS_3N) complex is dominating, as shown by the shift of the ^{113}Cd NMR signal upfield to 636 ppm. The mean Cd-S and Cd-(N/O) distances of 2.53 ± 0.02 and 2.28 ± 0.04 Å for solution **E2** are comparable to the corresponding average distances for the only structurally known cadmium(II) complex with CdS_3N configuration (2.522 and 2.207 Å) [*Supporting Material in* Ref. 33], and are consistent with our proposed structure **h** for the $[Cd(Cys)_3]^{4-}$ complex in Scheme 2. Formation of a $[Cd(Cys)_3]^{4-}$ complex with CdS_3N_2 coordination (Scheme S-1) can be excluded, since the average Cd-S and especially the Cd-(N/O) bond distances for solution **E2** are appreciably shorter than the mean Cd-S and Cd-N distances for five crystalline cadmium(II) complexes with CdS_3N_2 coordination (2.551 and 2.386 Å, respectively), which all are dinuclear complexes with long, bridging Cd-S bonds [*Supporting Material in* Ref. 33]. As a specific example, the Cd(cysteaminate)$_2$ complex with CdS_3N_2 coordination (solid state ^{113}Cd NMR δ_{iso} = 669 ppm) could be considered with one short (2.534 Å) Cd-S bond distance and two longer bridging Cd-S distances at 2.572 and 2.620 Å, and a mean Cd-N distance of 2.376 Å [45], which is ~ 0.1 Å longer than the mean Cd-(N/O) distances obtained for solution **E2**.

In solution **D1** (pH = 7.5) with δ(^{113}Cd) = 655 ppm the $[Cd(S\text{-cysteinate})_4]^{n-}$ complex is expected to be the dominating species as for **F2** and **G2**, together with a minor amount of $[Cd(cysteinate)_3]^{2-}$(CdS_3N) (**i** and **g** in Scheme 2). The EXAFS model fitting for solution **D1** resulted in similar residuals for three different models, i.e. CdS_4, CdS_3N and a mixture of CdS_4 + CdS_3N (50 : 50) (Table 3), all with the average Cd-S distance of 2.53 ± 0.02 Å.

Curve-fitting of the EXAFS spectra for solutions **B1** and **C1** (pH = 7.5), again resulted in the minimum residual for a single Cd-S shell model (Table 3); however, the ^{113}Cd chemical shifts of 585 - 627 ppm show that these solutions contain mixtures of cadmium(II)-cysteine complexes that are in equilibrium with intermediate ligand-exchange rate, with mainly CdS_3O and CdS_3N geometries (**f** and **g** in Scheme 2), for which the reported ranges of chemical shifts are 560 – 645 ppm and 637 - 659 ppm, respectively (Table 1). EXAFS model fitting using both Cd-S and Cd-(N/O) shells resulted in average bond distances of 2.54 ± 0.02 and 2.35 ± 0.04 Å, respectively (Table 3), which are close to the corresponding mean Cd-S and Cd-O distances, 2.53 and 2.30 Å, for the crystalline cadmium(II) complex (HIm)[Cd(tsac)$_3$(H_2O)], with CdS_3O coordination and a coordinated water molecule [40].

The ^{113}Cd chemical shifts for solutions **B2** – **G2** are generally lower than those of solutions **B1** – **G1** with comparable ligand / metal ratios (Figure 1). The partial protonation of the amine groups ($-NH_3^+$) in the solutions **B1** and **C1** at pH = 7.5, favors the formation of cadmium(II) cysteine complexes with CdS_3O coordination (from water). By increasing the cysteine concentration in the solutions **D1** – **G1**, another cysteine thiolate group can substitute the water and promote formation of the $[Cd(S\text{-cysteinate})_4]^{n-}$ complex. By raising the pH to 11.0, i.e. deprotonating all the amine groups, the chelate complexes $[Cd(S,N\text{-Cys})_2]^{2-}$ and $[Cd(Cys)_3]^{4-}$ (**e** and **h** in Scheme 2) gain stability, which is reflected in the lower chemical shifts for the alkaline solutions (**B2** – **G2**), relative to those at pH 7.5 (**B1** – **G1**). These species are in fast ligand-exchange equilibrium, resulting in a single averaged peak in NMR.

The curve-fitting of EXAFS models for solutions **A2** – **G2** and the corresponding Fourier-transforms are shown in Figure 3. For solutions **B2** – **E2**, where C_{H_2Cys} increases from 0.3 to 1.0 mol dm^{-3}, the refinement of the Cd-S contribution shows a gradual increase in the coordination number from N = 2.2 to 3.3 (Table 3), indicating an increasing concentration of the $[Cd(Cys)_3]^{4-}$ complex.

For solutions **A2** – **D2**, the Cd L_3-edge absorption spectra and their 2nd derivatives are intermediate to the spectra of $Cd(cysteaminate)_2$ (as CdS_3N_2 model) and bis(thiosaccharinato)-bis(imidazole) cadmium(II) $[Cd(tsac)_2(Im)_2]$ (as CdS_2N_2 model) (Figures 4 and S-4) [39, 40]. This is consistent with a mixture of $[Cd(Cys)_2]^{2-}$ and $[Cd(Cys)_3]^{4-}$ complexes in the solutions **A2** – **D2**. No standard complex with CdS_3N coordination was available for a more direct comparison.

Cadmium(II) Penicillamine Solutions

The ^{113}Cd chemical shifts for solutions **H1** and **H2** with C_{H_2Pen} = 0.2 mol·dm^{-3} are comparable (Figure 2) with those of corresponding cadmium(II) cysteine solutions **A1** and **A2** (Figure 1), and therefore, similar $CdS_2N(N/O)$ coordination environments are expected (like **c** – **e**, Scheme 2). The distribution diagram of the cadmium(II)-penicillamine complexes (Figure S-2a, *top left*) supports this conclusion, indicating that solution **H1** (pH = 7.5) contains a mixture of $[Cd(HPen)(Pen)]^-$ (CdS_2NO) and $[Cd(Pen)_2]^{2-}$ (CdS_2N_2) complexes, while in solution **H2** at pH = 11.0, the $[Cd(Pen)_2]^{2-}$ complex is the dominating species. This is also reflected in the broadness of ^{113}Cd NMR signals for **H1** and **H2**, where the broad signal for **H1** indicates an intermediate ligand-exchange between the cadmium(II) penicillamine complexes, and the narrow signal for **H2** is interpreted as an indication for presence of one dominating species.

For solution **H1** the EXAFS curve-fitting resulted in the minimum residual for a two-shell model. When the contribution of Cd-(N/O) path is fixed at *N* = 1.0, the Cd-S coordination number is refined to 2.7 (Table 4). For such a $CdS_3(N/O)$ coordination, however, a ^{113}Cd chemical shift higher than 560 ppm would be expected. A model with a fixed Cd-(N/O) contribution at 2.0 resulted in similar residual, and corresponds better to the observed $\delta(^{113}Cd)$ = 509 ppm. The average Cd-S and Cd-(N/O) bond distances 2.52 ± 0.02 and 2.30 ± 0.04 Å are slightly shorter than for the corresponding cysteine solution **A1** (2.54 ± 0.02 and 2.34 ± 0.04 Å), indicating stronger Cd-S bonding for the penicillamine complexes (like **c** – **e** in Scheme 1), a result of the inductive effect of the two methyl groups adjacent to the thiolate sulfur atom. When increasing the pH to 11.0 (solution **H2**), a good fit is obtained to the EXAFS oscillation for a model with two Cd-S distances at 2.50 ± 0.02 Å and two Cd-(N/O) at 2.30 ± 0.04 Å (Table 4). The similarity to the average Cd-S (2.473 Å) and Cd-N (2.288 Å) bond distances for ten crystalline CdS_2N_2 complexes [*Supporting Material in* Ref. 33], supports a dominating $[Cd(S,N\text{-Pen})_2]^{2-}$ complex in solution **H2**, with CdS_2N_2 coordination as for **e** in Scheme 2. In the corresponding cadmium(II)-cysteine solution **A2**, the average Cd-S bond distance of 2.53 ± 0.02 Å is somewhat longer.

For the solutions **L1** – **N1** (pH = 7.5) with large excess of penicillamine (C_{H_2Pen} ~ 0.87 - 1.0 mol dm^{-3}), the ^{113}Cd NMR chemical shifts are quite close, 602 – 607 ppm, in the ranges expected for CdS_3O and CdS_3N coordination (see Table 1), indicating mainly trithiolate $[Cd(penicillaminate)_3]^{m-}$ species with deprotonated $HPen^-$ or Pen^{2-} penicillamine ligands (similar to **f** and **g** in Scheme 2), for which no stability constants have been reported. These species are in fast ligand-exchange equilibrium. Their composition is probably comparable to that of the cadmium(II)-cysteine solution **C1** (Scheme 2), with a rather similar ^{113}Cd chemical shift of 627 ppm. The enhanced amplitude of the EXAFS oscillation for **L1** relative to **H1**, indicates an increase in the Cd-S coordination number (Figure S-7). EXAFS model fitting for the solution **L1** yielded average Cd-S and Cd-(N/O) distances of 2.53 ± 0.02 and 2.30 ± 0.04 Å, respectively (Table 4). For the only reported crystalline cadmium(II) complex with CdS_3N coordination,

the average bond distances are Cd-S 2.522 Å and Cd-N 2.207 Å [*Supporting Material in* Ref. 33], and for CdS_3O coordination in the thiosaccharinato complex (HIm)[$Cd(tsac)_3(H_2O)$], the mean bond distances are Cd-S 2.532 Å and Cd-O 2.304 Å [40], in very good agreement with those for **L1** (Table 4). Solutions **I1** – **K1** with chemical shifts (541 – 582 ppm) between those of **H1** and **N1** would contain mixtures of cadmium(II)-penicillamine complexes with $CdS_2(N/O)_2$ and $CdS_3(N/O)$ coordination, similar to **c** - **g** in Scheme 2, that are in ligand-exchange equilibrium with intermediate rate. EXAFS model fittings for solutions **I1 - K1** using different models, i.e. $CdS_3(N/O)$, $CdS_2(N/O)_2$ or a mixture of $CdS_2(N/O)_2$ + $CdS_3(N/O)$ (50 : 50), result in equally good fits, with the Cd-S distance 2.50 - 2.52 Å, and the Cd-(N/O) distance varying between 2.28 - 2.32 Å.

The stability constants reported by Avdeef *et al.* [16], propose polynuclear cadmium(II) penicillamine complexes in the pH range 4 - 8. According to the distribution diagram in Figure S-2b (*top left*), solution **H1** (pH 7.5) would contain almost equal amounts (~ 40%) of the $[Cd_3(HPen)_4(Pen)_2]^{2-}$ and $[Cd(Pen)_2]^{2-}$ (CdS_2N_2) complexes and a minor amount of the $[Cd_2(HPen)_3(Pen)_2]^{3-}$ complex. We expect that the polynuclear species would have structures similar to those shown in Scheme S-2 (see Supporting Information), with CdS_4 and/or $CdS_3(N/O)$ coordination site(s). However, polynuclear cadmium(II) complexes seem unlikely in this solution (**H1**) for the following reason. For the two bridged CdS_4 groups forming the dinuclear cadmium(II) binding site of the GAL4 protein [25], two ^{113}Cd NMR signals were observed at 669 and 707 ppm [26]. The reported ^{113}Cd chemical shifts for CdS_2N_2, CdS_3O and CdS_3N coordination are 519 ppm, 560 – 645 ppm and 637 – 659 ppm, respectively (Table 1). Thus, the expected $\delta(^{113}Cd)$ for a mixture of $[Cd(Pen)_2]^{2-}$ and $[Cd_3(HPen)_4(Pen)_2]^{2-}$ complexes should be close to ~ 600 ppm (for the coordination sites CdS_2N_2 + 2 × $CdS_3(N/O)$ + CdS_4) (similar to the $[Cd(HCys)_2]$ solid), rather than the experimental value of 509 ppm for solution **H1**.

By increasing the pH of the solutions containing a large excess of penicillamine to 11.0 in **L2 - N2** (C_{H2Pen} ~ 0.87 - 1.7 mol dm^{-3}), the ^{113}Cd chemical shifts become more shielded, moving to 575 - 578 ppm. Recently, chemical shifts of 574 – 588 ppm have been reported for a few members of the TRI family of peptides at pH 8.5 – 9.5, and were attributed to CdS_3O coordination [27-29]. In an earlier study on cadmium(II) thiolate complexes [46], ^{113}Cd chemical shifts of 623 and 577 ppm were observed for alkaline cadmium(II) cysteine and penicillamine solutions (pH = 13, $C_{Cd(II)}$ = 0.05 mol dm^{-3}, C_{H2L} / $C_{Cd(II)}$ = 12). While the former value was attributed to the formation of the tetra-thiolate $[Cd(Cys)_4]^{6-}$ complex, the upfield shift of the corresponding penicillamine solution was interpreted as a result of the steric effect from the methyl groups, preventing ligation through the sulfur atom alone [46], or causing weaker Cd-S bonding and therefore poorer deshielding of the thiolate groups [18].

We may interpret the ^{113}Cd chemical shifts of **L2** – **N2** in two different ways: 1) either these solutions exclusively contain the $[Cd(S\text{-}Pen)_3]^{4-}$ complex with CdS_3O coordination, where the O-donor ligand is water (or OH^-); or 2) a mixture of $[Cd(Pen)_2]^{2-}$ (CdS_2N_2) and $[Cd(Pen)_3]^{4-}$ (CdS_3N) complexes are present in a fast ligand-exchange equilibrium. In the first case the downfield shift of the NMR signal to 602 – 607 ppm for the corresponding **L1** – **N1** solutions would be difficult to explain. If we assume that the solutions **L2** – **N2** would contain the $[Cd(Pen)_3(H_2O)]^{4-}$ (CdS_3O) complex, the composition should not change at pH = 7.5, when most of the coordinated cysteine amine groups are protonated. Assuming the existence of a hydroxo complex $[Cd(Pen)_3(OH)]^{5-}$ (CdS_3O) in alkaline solutions **L2** – **N2** (as shown in Figure S-2a, b), would require a hydrated $[Cd(Pen)_3(H_2O)]^{4-}$ complex at pH = 7.5. Since H_2O is a more shielding ligand than OH^- [47], the NMR signal for $[Cd(Pen)_3(H_2O)]^{4-}$ would be more shielded than for $[Cd(Pen)_3(OH)]^{5-}$ in alkaline solution. However, this is opposite to the observed trend for the ^{113}Cd chemical shift for solution **L1** (pH 7.5), which is more deshielded than **L2** (pH 11.0). Hence, a hydroxo complex in **L2** does not seem to be feasible, and therefore,

we conclude that the solutions **L2** – **N2** ($C_{H_2Pen} \geq 0.9$ mol dm^{-3}) contain mixtures of [Cd(Pen)$_2$]$^{2-}$ and [Cd(Pen)$_3$]$^{4-}$ complexes, similar to the cadmium(II) – cysteine solution **C2** with a ^{113}Cd NMR chemical shift of 577 ppm (see Figure 1 and **e**, **h** in Scheme 2).

The EXAFS spectra of solutions **L2** - **N2** almost overlap (Figure S-8), as would be expected from the similarity of their ^{113}Cd NMR spectra. The single-shell Cd-S model refinements of these spectra resulted in coordination numbers between 3.0 - 3.4 and a mean Cd-S distance of 2.51 ± 0.02 Å, which is longer than the average Cd-S bond distance in the crystalline trithiolate CdS_3 complexes (2.446 Å; *Supporting Material in* Ref. 33). Adding Cd-(N/O) backscattering to the fitting model slightly improved the residual for **L2** and **M2**. The model fitted to the EXAFS spectra of solutions **L2** - **N2**, assuming a 50:50 mixture of the [Cd(Pen)$_2$]$^{2-}$ (CdS_2N_2) and [Cd(Pen)$_3$]$^{4-}$ (CdS_3N) complexes by fixing the coordination numbers to $CdS_{2.5}N_{1.5}$, resulted in mean Cd-S and Cd-(N/O) distances of 2.52 ± 0.02 and 2.31 - 2.33 Å, respectively (Table 4).

The ^{113}Cd chemical shifts for **M1** and **N1** (604 - 607 ppm) are upfield relative to those of the corresponding cadmium(II) –cysteine solutions **F1** and **G1** (679 – 680 ppm) with similar ligand / metal mole ratios (C_{H_2Cys} / $C_{Cd(II)}$ = 15 – 20). This upfield shift is probably an effect of the steric hindrance from the two methyl groups close to the thiolate group, preventing the formation of [Cd(*S*-penicillamine)$_4$]$^{n-}$ (CdS_4) species in these solutions. We also observe that the ^{113}Cd chemical shifts for the cadmium(II) cysteine solutions **F2** and **G2** at pH 11.0 (654 – 658 ppm), are considerably more deshielded than those of the corresponding penicillamine solutions **M2** and **N2** (578 ppm). According to the Cd L$_3$-edge XANES spectra, the solutions **F2** and **G2** with comparable ligand excess ($C_{H_2Cys} \geq 1.5$ mol dm^{-3}) mainly contain the [Cd(Cys)$_4$]$^{6-}$ complex, possibly with some minor amount of [Cd(Cys)$_3$]$^{4-}$ but not [Cd(Cys)$_2$]$^{2-}$. One reason is the fact that the cysteine thiolate group does not experience the steric hindrance problem that the penicillamine thiolate has. Therefore, in the presence of an excess amount of cysteine in the solution the formation of cadmium(II) complexes with higher thiolate coordination number is facilitated. Another reason is probably related to the lower stability of the [Cd(Cys)$_2$]$^{2-}$ complex in comparison with [Cd(Pen)$_2$]$^{2-}$, as indicated by its slightly shorter mean Cd-S bond distance, 2.50 ± 0.02 Å (solution **H2**) vs. 2.53 ± 0.02 Å for [Cd(Cys)$_2$]$^{2-}$ (in solution **A2**); see Tables 3 and 4.

Conclusion

The cadmium(II) complex formation with cysteine or penicillamine (3, 3′-dimethylcysteine) has been studied at the pH values (7.5 and 11.0) using ^{113}Cd NMR and Cd K and L$_3$-edge X-ray absorption spectroscopy, for solutions with $C_{Cd(II)} \sim 0.1$ mol dm^{-3} and ligand / metal mole ratios varied from C_{H_2L} / $C_{Cd(II)}$ = 2.0 to 20. At C_{H_2L} / $C_{Cd(II)}$ = 2.0 both ligands form complexes with distorted tetrahedral CdS_2N(N/O) coordination geometries, which correspond to a single ^{113}Cd NMR resonance at 509 – 527 ppm. For the [Cd(cysteinate)$_2$]$^{k-}$ species at pH 7.5, the average Cd-S and Cd-(N/O) bond distances from Cd K-edge EXAFS spectra, 2.54 ± 0.02 and 2.34 ± 0.04 Å, respectively, show a slight tendency to become shorter for the dominating [Cd(*S*,*N*-Cys)$_2$]$^{2-}$ complex formed when the amine groups deprotonate at pH = 11.0, to 2.53 ± 0.02 and 2.29 ± 0.04 Å. The [Cd(*S*,*N*-Pen)$_2$]$^{2-}$ complex that forms in the corresponding penicillamine solution at pH 11.0 has a slightly shorter Cd-S bond distance, 2.50 ± 0.02 Å, but the Cd-(N/O) distance remains similar, 2.30 ± 0.04 Å.

For solutions with higher ligand concentration, the ^{113}Cd resonances shift downfield, which indicates an increasing number of thiolate ligands in the cadmium(II) complexes. For solutions containing a large excess of cysteine (C_{H_2Cys} / $C_{Cd(II)}$ = 10 – 20), the ^{113}Cd chemical shifts of ~ 680 ppm at pH = 7.5, and the average Cd-S bond distance of 2.53 ± 0.02 Å, were attributed to a predominant [Cd(*S*-cysteinate)$_4$]$^{n-}$ complex, with the cysteine ligands in HCys$^-$ or Cys^{2-}

forms. The average Cd-S distance does not change at pH = 11, and the Cd L_3-edge XANES spectra for alkaline solutions with C_{H_2Cys} / $C_{Cd(II)}$ = 15 – 20 show similar features as in the spectrum of the CdS_4 model compound. However, the ^{113}Cd resonances of the solutions shift upfield to 636 - 658 ppm, indicating that when all thiol and amine groups of the cysteine ligands are deprotonated a minor amount of the $[Cd(Cys)_3]^{4-}$ (CdS_3N) complex is present together with the dominating $[Cd(Cys)_4]^{6-}$ complex in these solutions.

For cadmium(II)-penicillamine solutions with similar ligand excess, at pH 7.5 the average Cd-S and Cd-(N/O) bond distances are 2.53 ± 0.02 and 2.30 ± 0.04 Å (for C_{H_2Pen} / $C_{Cd(II)}$ = 10), while their ^{113}Cd resonance (at ~ 600 ppm) indicates that $[Cd(penicillaminate)_3]^{m-}$ complexes with CdS_3(N/O) geometry are dominating. That upfield shift of ~ 80 ppm relative to the corresponding cadmium(II)-cysteine solutions is probably an effect of the steric hindrance by the two methyl groups in penicillamine, which obstructs formation of the $[Cd(S\text{-penicillaminate})_4]^{n-}$ complex. At pH = 11.0, the average Cd-S bond distances remain unchanged, while the ^{113}Cd chemical shifts are found to be ~ 578 ppm. Those signals, again about 60 – 80 ppm upfield relative to similar cadmium(II)-cysteine solutions, indicate that these solutions contain a mixture of $[Cd(Pen)_3]^{4-}$ and $[Cd(S,N\text{-Pen})_2]^{2-}$ complexes, with the latter being more stable than the corresponding $[Cd(S,N\text{-Cys})_2]^{2-}$ complex, consistent with its shorter Cd-S bond distance (see above).

The differences revealed between cysteine and penicillamine as ligands to cadmium(II) ions in the present study can be linked to the fact that the toxicity of cadmium(II) is reduced when captured *in vivo* by cysteine-rich metallothionines in CdS_4 coordination sites, while penicillamine, which has been clinically used for treating the toxic effects of mercury(II) and lead(II) exposure, is not an efficient antidote against cadmium(II) poisoning.

Supplementary Material

Refer to Web version on PubMed Central for supplementary material.

Acknowledgments

We are grateful to Qiao Wu and Dorothy Fox at the instrument facility at the Department of Chemistry, University of Calgary, for their skilful assistance in measuring the NMR spectra. Beamtime was allocated for X-ray absorption measurements at the Photon Factory, Tsukuba, Japan (proposal No. 2005G226), and SSRL (proposal No. 2848), which is operated by the Department of Energy, Office of Basic Energy Sciences, USA. The SSRL Biotechnology Program is supported by the National Institutes of Health, National Center for Research Resources, Biomedical Technology Program, and by the Department of Energy, Office of Biological and Environmental Research. We gratefully acknowledge the Natural Sciences and Engineering Research Council (NSERC) of Canada, Canadian Foundation for Innovation (CFI), Alberta Science and Research Investments Program (ASRIP), Alberta Synchrotron Institute (ASI) and the University of Calgary for providing financial support. F.J. is recipient of NSERC University Faculty Award (UFA).

References

1. Deckert J. Biometals 2005;18:475–481. [PubMed: 16333748]
2. Lane TW, Saito MA, George GN, Pickering IJ, Prince RC, Morel FFM. Nature 2005;435:42. [PubMed: 15875011]
3. Lane TW, Morel FMM. Proc Natl Acad Sci USA 2000;97:4627–4631. [PubMed: 10781068]
4. Ishihara T, Kobayashi E, Okubo Y, Suwazono Y, Kido T, Nishijyo M, Nakagawa H, Nogawa K. Toxicology 2001;163:23–28. [PubMed: 11376862]
5. Shaikh ZA, Vu TT, Zaman K. Toxicol Appl Pharmacol 1999;154:256–263. [PubMed: 9931285]
6. Vašák M, Kägi JHR, Hill HAO. Biochemistry 1981;20:2852–2856. [PubMed: 7248252]
7. Boulanger Y, Goodman CM, Forte CP, Fesik SW, Armitage IM. Proc Natl Acad Sci USA 1983;80:1501–1505. [PubMed: 6572910]

8. Henkel G, Krebs B. Chem Rev 2004;104:801–824. [PubMed: 14871142]
9. Goyer RA, Miller CR, Zhu SY, Victery W. Toxicol Appl Pharmacol 1989;101:232–244. [PubMed: 2815080]
10. Fotakis G, Timbrell JA. Toxicol in Vitro 2006;20:641–648. [PubMed: 16442773]
11. Shibasaki T, Matsumoto H, Gomi H, Ohno I, Ishimoto F, Sakai O. Biol Trace Elem Res 1996;52:1–9. [PubMed: 8860661]
12. Berthon G. Pure Appl Chem 1995;67:1117–1240.
13. Bottari E, Festa MR. Talanta 1997;44:1705–1718. [PubMed: 18966910]
14. Cole A, Furnival C, Huang ZX, Jones DC, May PM, Smith GL, Whittaker J, Williams DR. Inorg Chim Acta 1985;108:165–171.
15. Corrie MA, Walker MD, Williams DR. J Chem Soc Dalton Trans 1976:1012–1015.
16. Avdeef A, Kearney DL. J Am Chem Soc 1982;104:7212–7218.
17. Öz G, Pountney DL, Armitage IM. Biochem Cell Biol 1998;76:223–234. [PubMed: 9923691]
18. Summers MF. Coord Chem Rev 1988;86:43–134.
19. Eichele K, Wasylishen RE. Inorg Chem 1994;33:2766–2773.
20. Bobsein BR, Myers RJ. J Am Chem Soc 1980;102:2454–2455.
21. Henehan CJ, Pountney DL, Zerbe O, Vašák M. Protein Sci 1993;2:1756–1764. [PubMed: 8251947]
22. Lee HJ, Lian LY, Scrutton NS. Biochem J 1997;328:131–136. [PubMed: 9359843]
23. Pan T, Freedman LP, Coleman JE. Biochemistry 1990;29:9218–9225. [PubMed: 2271590]
24. Luczkowski M, Stachura M, Schirf V, Demeler B, Hemmingsen L, Pecoraro VL. Inorg Chem 2008;47:10875–10888. [PubMed: 18959366]
25. Baleja JD, Marmorstein R, Harrison SC, Wagner G. Nature 1992;356:450–453. [PubMed: 1557130]
26. Gardner KH, Pan T, Narula S, Rivera E, Coleman JE. Biochemistry 1991;30:11292–11302. [PubMed: 1958667]
27. Lee KH, Cabello C, Hemmingsen L, Marsh ENG, Pecoraro VL. Angew Chem Int Ed 2006;45:2864–2868.
28. Iranzo O, Cabello C, Pecoraro VL. Angew Chem Int Ed 2007;46:6688–6691.
29. Peacock AFA, Hemmingsen L, Pecoraro VL. Proc Natl Acad Sci USA 2008;105:16566–16571. [PubMed: 18940928]
30. Li X, Suzuki K, Kanaori K, Tajima K, Kashiwada A, Hiroaki H, Kohda D, Tanaka T. Protein Sci 2000;9:1327–1333. [PubMed: 10933497]
31. Pickering IJ, Prince RC, George GN, Rauser WE, Wickramasinghe WA, Watson AA, Dameron CT, Dance IG, Fairlie DP, Salt DE. Biochim Biophys Acta 1999;1429:351–364. [PubMed: 9989220]
32. Isaure MP, Fayard B, Sarret G, Pairis S, Bourguignon J. Spectrochim Acta B 2006;61:1242–1252.
33. Jalilehvand F, Mah V, Leung BO, Mink J, Hajba L. Inorg Chem. 2009 in press.
34. Jalilehvand F, Leung BO, Izadifard M, Damian E. Inorg Chem 2006;45:66–73. [PubMed: 16390041]
35. Ressler T. J Synchrotron Rad 1998;5:118–122.
36. Zabinsky SI, Rehr JJ, Ankudinov A, Albers RC, Eller MJ. Phys Rev B 1995;52:2995–3009.
37. Ankudinov AL, Rehr JJ. Phys Rev B 1997;56:R1712–R1716.
38. Ravel B. J Synchrotron Rad 2001;8:314–316.
39. Bharara MS, Kim CH, Parkin S, Atwood DA. Polyhedron 2005;24:865–871.
40. Tarulli SH, Quinzani OV, Baran EJ, Piro OE, Castellano EE. J Mol Struct 2003;656:161–168.
41. Maitani T, Suzuki KT. Inorg Nuclear Chem Lett 1979;15:213–217.
42. Darensbourg DJ, Niezgoda SA, Draper JD, Reibenspies JH. J Am Chem Soc 1998;120:4690–4698.
43. Hemmingsen L, Olsen L, Antony J, Sauer SPA. J Biol Inorg Chem 2004;9:591–599. [PubMed: 15221483]
44. Maher M, Cross M, Wilce MCJ, Guss JM, Wedd AG. Acta Cryst 2004;D60:298–303.
45. Fleischer H, Dienes Y, Mathiasch B, Schmitt V, Schollmeyer D. Inorg Chem 2005;44:8087–8096. [PubMed: 16241159]
46. Carson GK, Dean PAW, Stillman MJ. Inorg Chim Acta 1981;56:59–71.

47. Jonsson NBH, Tibell LAE, Evelhoch JL, Bell SJ, Sudmeier JL. Proc Natl Acd Sci USA 1980;77:3269–3272.

48. Xiao Z, Lavery MJ, Ayhan M, Scrofani SDB, Wilce MCJ, Guss JM, Tregloan PA, George GN, Wedd AG. J Am Chem Soc 1998;120:4135–4150.

49. Giedroc DP, Johnson BA, Armitage IM, Coleman JE. Biochemistry 1989;28:2410–2418. [PubMed: 2659069]

50. Roberts WJ, Pan T, Elliott JI, Coleman JE, Williams KR. Biochemistry 1989;28:10043–10047. [PubMed: 2695161]

51. South TL, Kim B, Summers MF. J Am Chem Soc 1989;111:395–396.

52. Fitzgerald DW, Coleman JE. Biochemistry 1991;30:5195–5201. [PubMed: 2036385]

53. Bobsein BR, Myers RJ. J Biol Chem 1981;256:5313–5316. [PubMed: 7016851]

54. Meijers R, Morris RJ, Adolph HW, Merli A, Lamzin VS, Cedergren-Zeppezauer ES. J Biol Chem 2001;276:9316–9321. [PubMed: 11134046]

55. Engeseth HR, McMillin DR, Otvos JD. J Biol Chem 1984;259:4822–4826. [PubMed: 6232270]

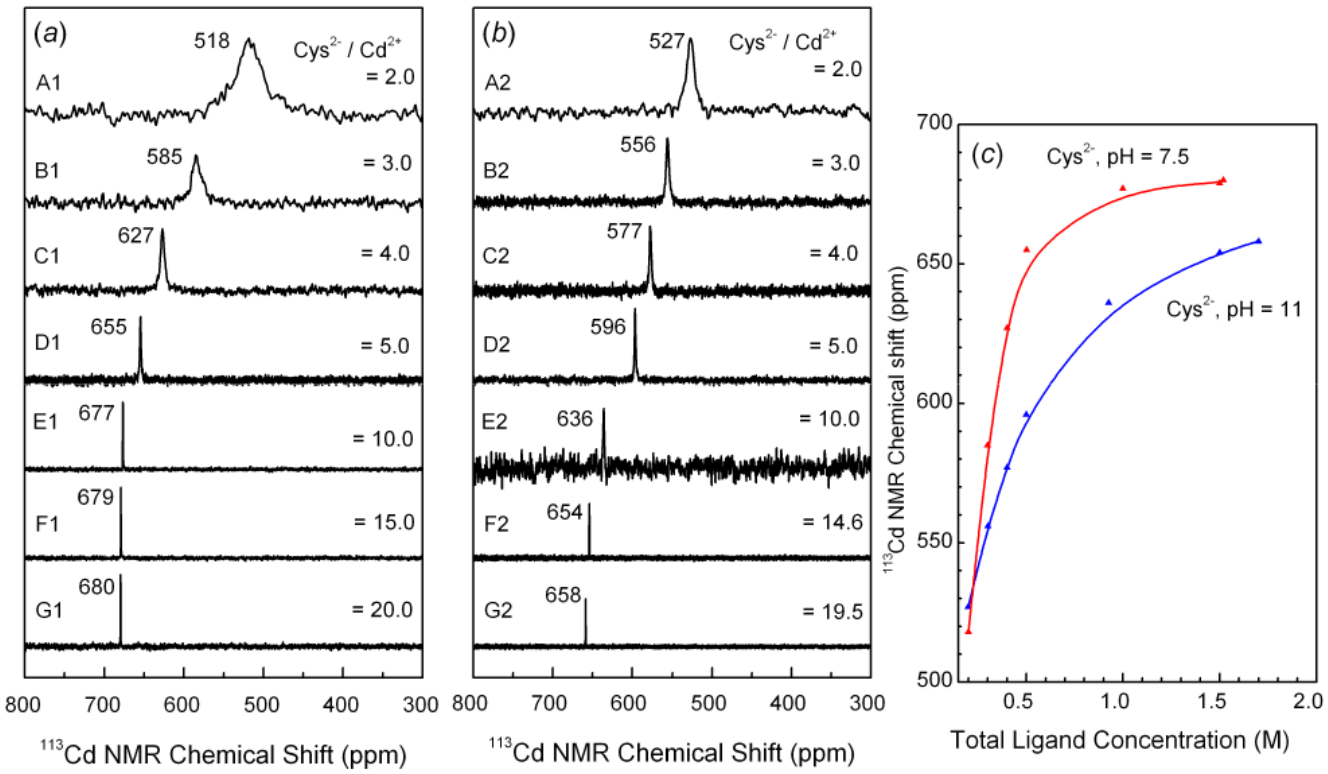

Figure 1.

^{113}Cd NMR spectra of ~ 0.1 mol·dm^{-3} cadmium(II) solutions with increasing amount of cysteine at pH 7.5 (*left*) and 11 (*middle*). The variation of the ^{113}Cd chemical shift *vs*. total cysteine concentration is shown to the right.

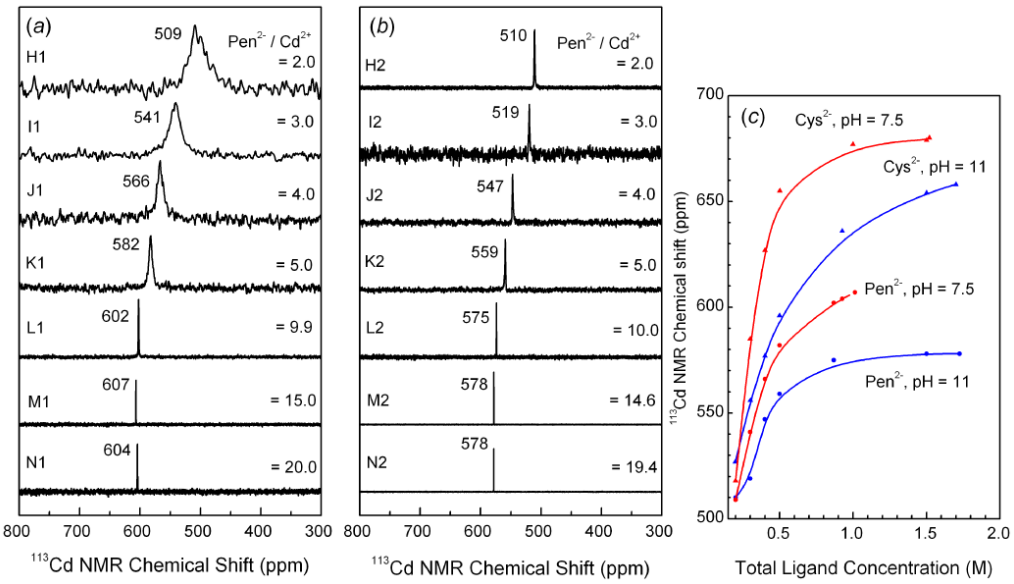

Figure 2.

^{113}Cd NMR spectra of cadmium(II) penicillamine solutions at pH 7.5 (*left*) and 11 (*middle*). The variation of the ^{113}Cd chemical shift for cadmium(II) cysteine and penicillamine solutions *vs*. total ligand concentration is shown to the right.

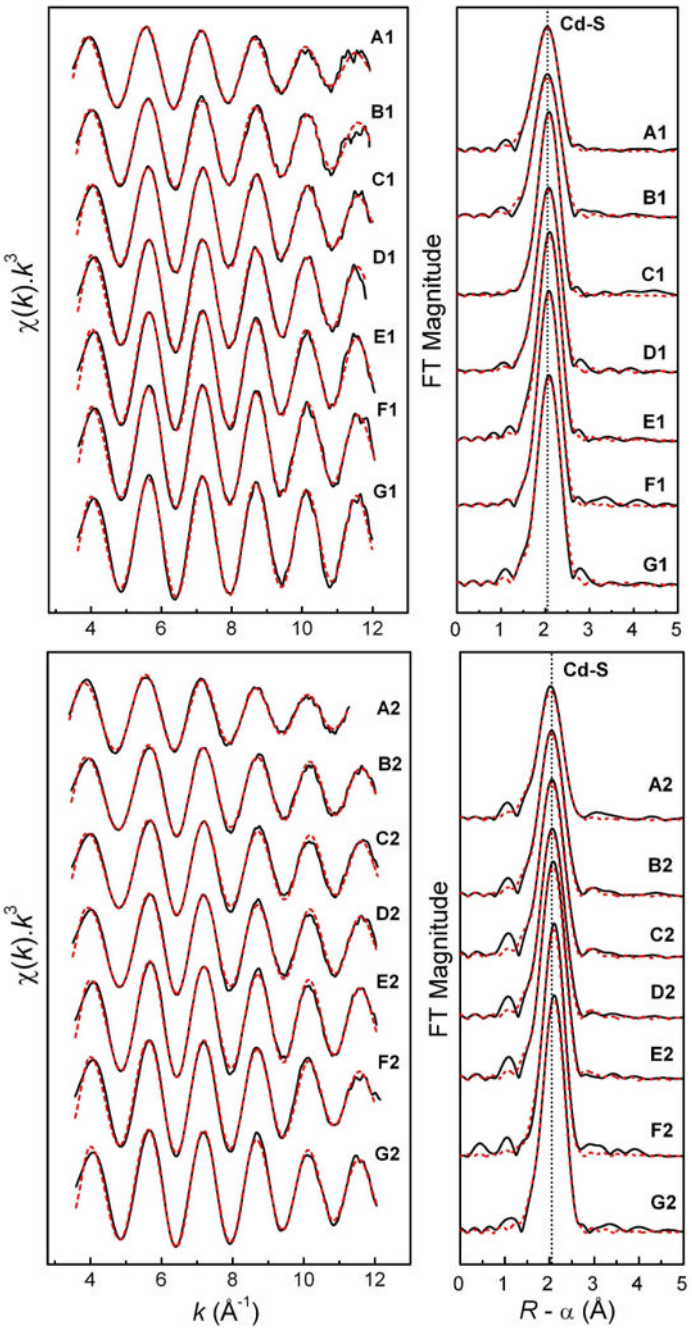

Figure 3.

Least-squares curve-fitting of k^3-weighted Cd K-edge EXAFS spectra of the cadmium(II)-cysteine solutions at pH = 7.5 (**A1 – G1**) and pH = 11.0 (**A2 – G2**), and the corresponding Fourier-transforms, using a model containing both Cd-S and Cd-(N/O) paths (see Table 3).

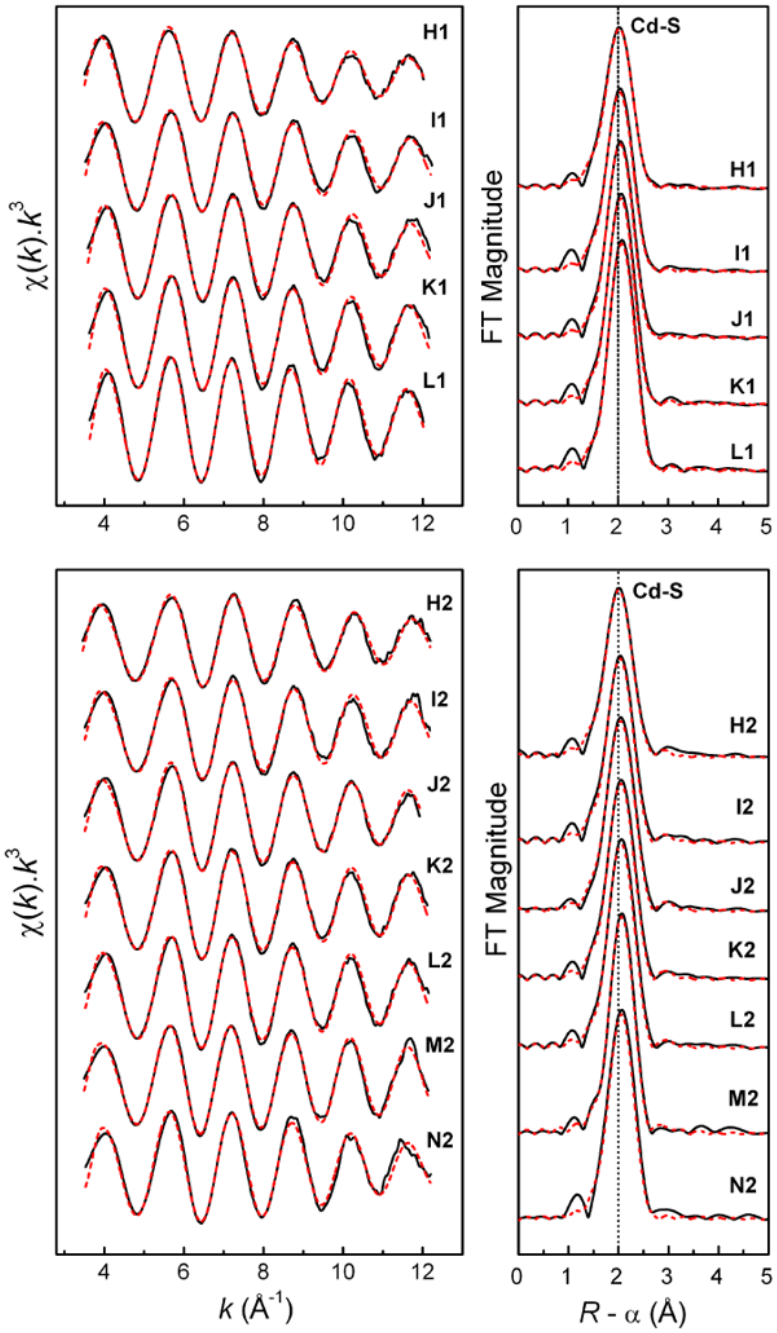

Figure 4.

Least-squares curve-fitting of k^3-weighted Cd K-edge EXAFS spectra of cadmium(II)-penicillamine solutions at pH = 7.5 (**H1** – **L1**) and pH = 11.0 (**H2** – **N2**), and the corresponding Fourier-transforms (see Table 4).

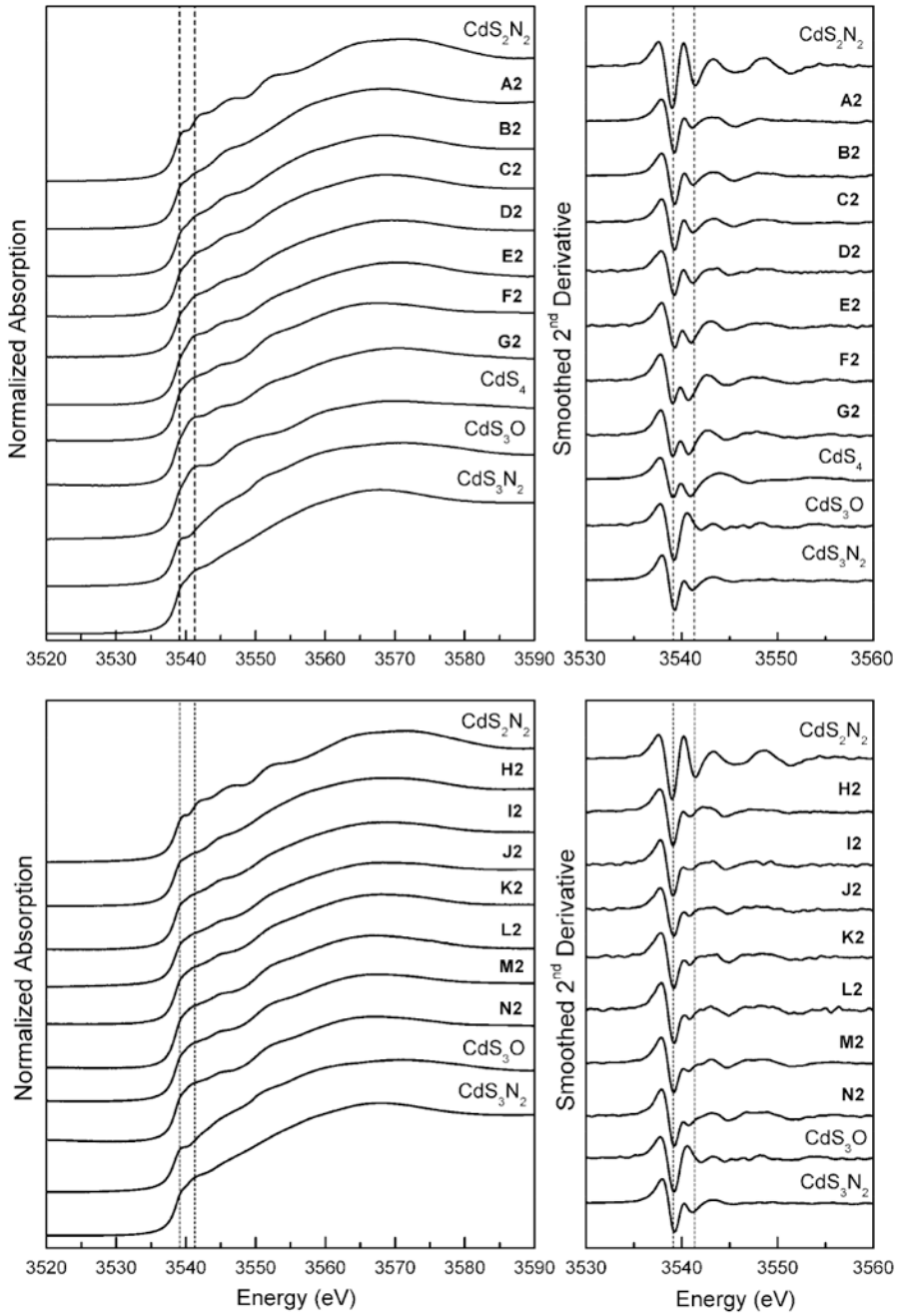

Figure 5.

Normalized Cd L_3-edge XANES spectra and corresponding smoothed 2nd derivatives for the cadmium(II)-cysteine (**A2 – G2**) and cadmium(II)-penicillamine (**H2 – N2**) solutions (pH = 11.0), and for crystalline compounds with $CdS_x(N/O)_y$ coordination (Ref. 33). Dashed lines are at 3539.1 and 3541.3 eV.

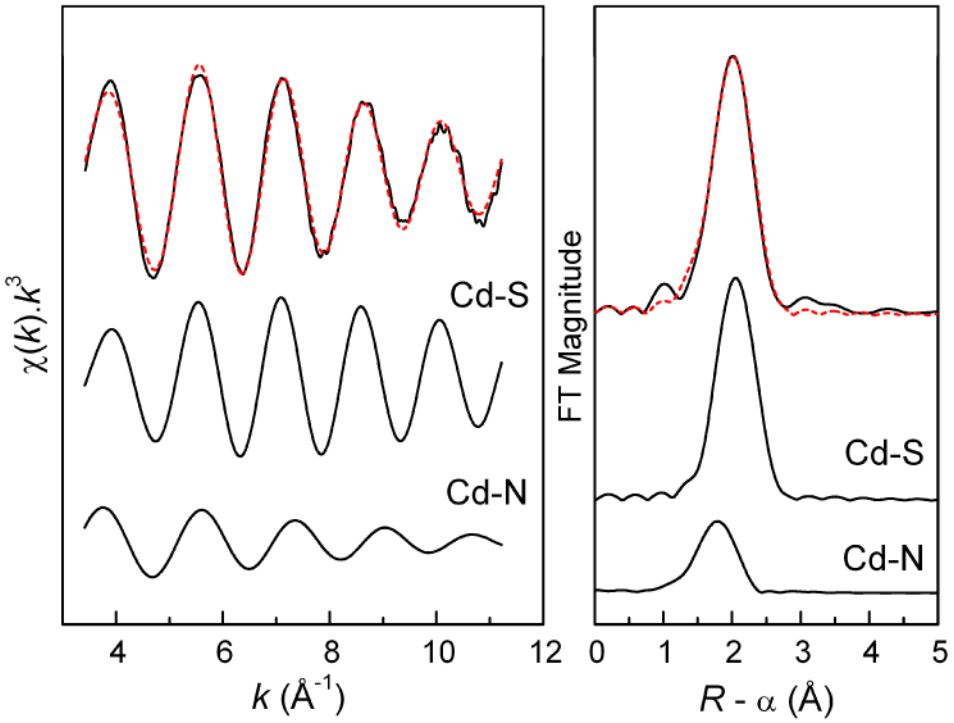

Figure 6.

Least-squares k^3-weighted curve fitting for a CdS_2N_2 coordination model to the Cd K-edge EXAFS oscillation of the cadmium(II) cysteine solution **A2** (pH = 11.0) and the corresponding Fourier-transform (solid line, exp.; red dash line, fit), with the separate contributions below (see Table 3).

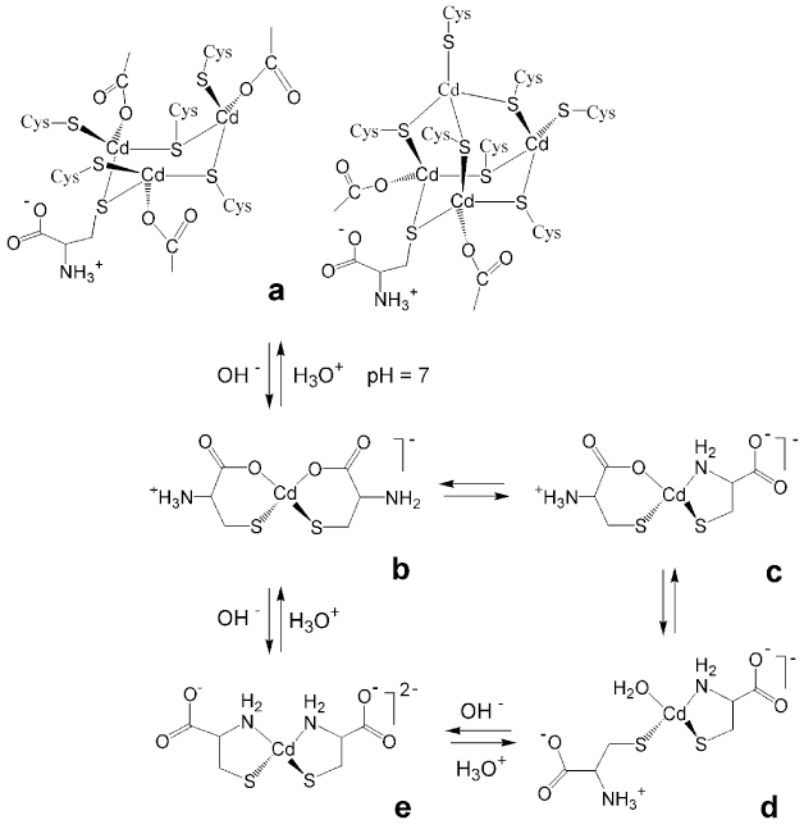

Scheme 1.

Transformations between possible types of coordination for mononuclear cadmium(II)-cysteine $[Cd(HCys)(Cys)]^-$ (**b** – **d**) and $[Cd(Cys)_2]^{2-}$ (**e**) complexes. The species **c** - **e** with $CdS_2N(N/O)$ coordination may exist in comparable amount in solution **A1** (pH 7.5), prepared by dissolving the solid $Cd(HCys)_2 \cdot H_2O$ compound. Structures (**a**) are two of the possible structures for this compound (Ref. 33), with the coordinated COO^- groups from cysteine ligands.

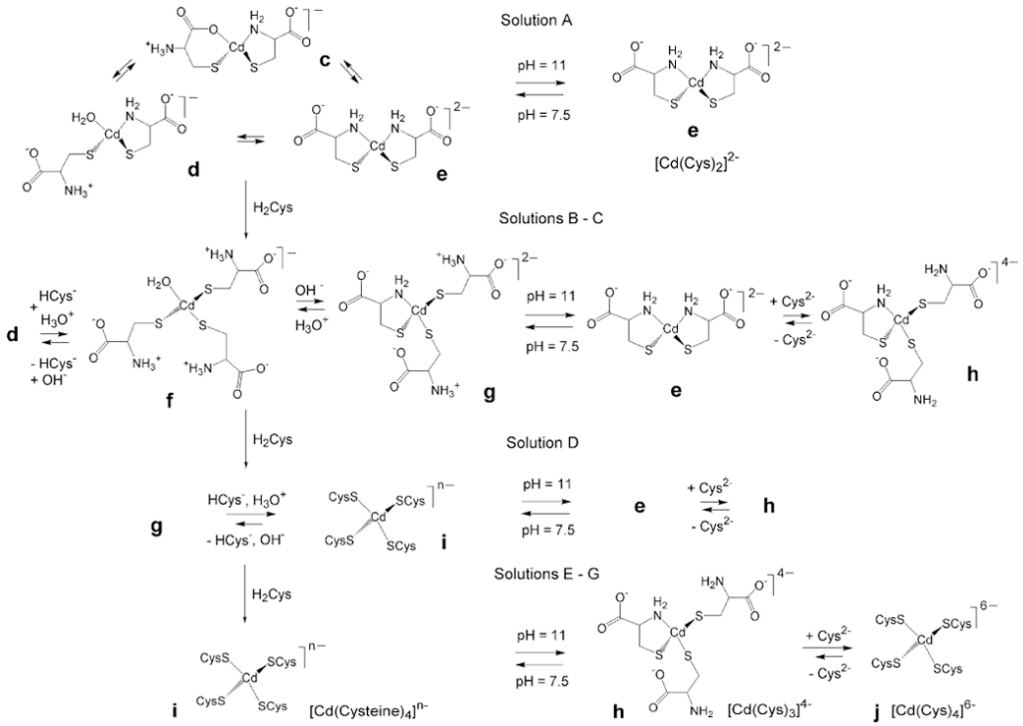

Scheme 2.

An overview of the dominating mononuclear species present in the cadmium(II)-cysteine solutions (**A** – **G**) at pH 7.5 and 11.0.

Table 1

Reported ^{113}Cd chemical shifts for biologically relevant, mononuclear cadmium(II)-thiolate coordination sites.

	Chemical shift (δ, ppm)	Ref.
CdS_4	650, 680, 704 – 751	[20,21-24]
CdS_3	572, 684 - 690	[27-30]
CdS_3O	560 - 645	[24,27-29,48]
CdS_3N	637 - 659	[49-52]
CdS_3N_2[a]	669	[39]
CdS_2N_2	519	[20]
CdS_2NO_w[b]	483	[20]
CdS_2NO_2	442	[53,54]
$CdSS^*N_2$[c]	432	[55]

[a] Solid state NMR for cadmium(II)-cysteaminate (CdS_3N_2)

[b] O_W, water

[c] S*, thioether or disulfide.

Table 2

Composition of the cadmium(II)-cysteine and penicillamine solutions.[a]

Solution	H_2L/Cd^{II} ratio	$[Cd^{2+}]_{tot}$ [b]	$[H_2L]_{tot}$	pH	Solution	H_2L/Cd^{II} ratio	$[Cd^{2+}]_{tot}$ [b]	$[H_2L]_{tot}$	pH
L = Cys									
A1	2.0	100	200	7.5	A2	2.0	100	200	11.0
B1	3.0	100	300	7.5	B2	3.0	99	301	11.0
C1	4.0	100	401	7.5	C2	4.0	100	400	11.1
D1	5.0	100	500	7.5	D2	5.0	99	499	11.0
E1	10.0	100	1000	7.5	E2	10.1	92	927	10.9
F1	15.0	100	1498	7.5	F2	14.6	103	1500	11.1
G1	19.9	76	1513	7.5	G2	19.5	93	1818	11.1
L = Pen									
H1	2.0	100	200	7.5	H2	2.0	100	200	11.3
I1	3.0	100	301	7.6	I2	3.0	100	299	11.1
J1	4.0	100	399	7.5	J2	4.0	100	399	11.0
K1	5.0	100	500	7.4	K2	5.0	100	500	11.0
L1	10.0	87	867	7.5	L2	10.0	87	869	11.0
M1	14.9	68	1014	7.5	M2	14.6	103	1501	11.0
N1	20.1	46	926	7.5	N2	19.4	89	1725	11.0

[a] Concentrations in $mmol \cdot dm^{-3}$

[b] The $[Cd^{2+}]_{tot}$ concentrations are within ± 3 $mmol \cdot dm^{-3}$, according to the ICP analysis.

Table 3

Cd K-edge EXAFS data analysis for cadmium(II) cysteine solutions at pH = 7.5 (A1 – G1) and pH = 11.0 (A2 – G2, see Figure 3).[a]

Solution	^{113}Cd NMR (δ, ppm)	Cd-S			Cd-(N/O)			R^b
		N	*R* (Å)	σ² (Å²)	*N*	*R* (Å)	σ² (Å²)	
A1	518	3.6	2.52	0.0080				13.0
		2.5	2.54	0.0056	1 *f*	2.30	0.0053	13.8
		1.9	**2.54**	0.0047	2 *f*	**2.34**	0.0065	13.7 (*)
B1	585	3.6	2.52	0.0065				12.8
		2.8	**2.54**	0.0058	1 *f*	**2.35**	0.0031	13.2 (*)
		2.1	2.55	0.0050	2 *f*	2.36	0.0043	13.7
C1	627	3.7	2.52	0.0056				9.3
		3.7	2.52	0.0069	1 *f*	2.41	0.0016	9.3
		3 *f*	**2.54**	0.0050	0.9	**2.35**	0.0030	9.5 (*)
D1	655	3.9	**2.53**	0.0055				10.2 (*)
		2.7	2.54	0.0033	1 *f*	2.31	0.0012	10.6[c]
		3.5 *f*	2.53	0.0049	0.5 *f*	2.31	0.0036	10.5
E1	677	4.1	**2.53**	0.0053				9.9 (*)
		3.0	2.54	0.0031	1 *f*	2.30	0.0018	10.2[c]
		3 *f*	2.54	0.0030	0.8	2.29	0.0001	10.0[c]
F1	679	4.0	**2.52**	0.0049				10.4 (*)
		4.0	2.53	0.0068	1 *f*	2.39	-0.0010	9.5[c]
		3 *f*	2.55	0.0056	2.0	2.38	0.0014	10.1[c]
G1	680	3.8	**2.53**	0.0042				12.5 (*)
		3.3	2.53	0.0035	1 *f*	2.32	0.0111	12.6[c]
		3 *f*	2.54	0.0029	1.1	2.31	0.0065	12.9[c]
A2	527	3.9	2.52	0.0095				13.3
		3.2	2.52	0.0076	1 *f*	2.20	0.0114	11.3
		2.9	2.52	0.0072	2 *f*	2.25	0.0199	11.3
		2 *f*	**2.53**	0.0049	2 *f*	**2.29**	0.0094	12.5 (*)
B2	556	3.3	2.51	0.0063				12.6

Solution	^{113}Cd NMR (δ, ppm)	Cd-S			Cd-(N/O)			R^b
		N	*R* (Å)	σ² (Å²)	*N*	*R* (Å)	σ² (Å²)	
		2.5	2.51	0.0043	1 *f*	2.25	0.0063	10.3
		2.2	**2.52**	0.0040	2 *f*	**2.30**	0.0119	10.5 (*)
C2	576	3.4	2.51	0.0059				13.0
		2.8	2.51	0.0045	1 *f*	2.24	0.0093	11.2
		2.6	2.52	0.0045	2 *f*	2.30	0.0179	10.5
		2.5 *f*	**2.52**	0.0041	1.5 *f*	**2.27**	0.0116	11.2 (*)
D2	596	3.5	2.52	0.0057				9.5
		2.9	**2.52**	0.0047	1 *f*	**2.28**	0.0122	9.0 (*)
E2	636	3.9	2.53	0.0054				9.7
		3.3	**2.53**	0.0044	1 *f*	**2.28**	0.0107	9.2 (*)
F2	654	4.1	**2.53**	0.0060				9.1 (*)
		3.2	2.54	0.0047	1 *f*	2.33	0.0030	8.3[c]
G2	658	3.9	**2.53**	0.0052				8.3 (*)
		2.9	2.54	0.0035	1 *f*	2.31	0.0030	8.3[c]

[a] (*) fits that are compatible with the observed ^{113}Cd NMR chemical shifts and shown in Figure 3; *f* = fixed; S_0^2 = 0.87 *f; N* = coordination number/ frequency; *k*-fitting range = 3.5 - 12.0 Å^{-1} (11.2 Å^{-1} for **A2**);

[b] The residual (%) from the least-squares curve fitting is defined as: $$\frac{\sum_{i=1}^{N} \left| y_{\mathrm{exp}}(i) - y_{\mathrm{theo}}(i) \right|}{\sum_{i=1}^{N} \left| y_{\mathrm{exp}}(i) \right|} \times 100$$ where y_{exp} and y_{theo} are experimental and theoretical data points, respectively.

[c] Attempts to introduce a Cd-(N/O) contribution in the model.

Table 4

Cd K-edge EXAFS data analysis for cadmium(II) penicillamine solutions at pH = 7.5 (**H1-L1**) and pH = 11.0 (**H2 - N2**, see Figure 4)[a, b]

Solution	^{113}Cd NMR (δ, ppm)	Cd-S			Cd-(N/O)			R^c
		N	*R* (Å)	σ² (Å²)	*N*	*R* (Å)	σ² (Å²)	
H1	509	3.7	2.50	0.0081				11.8
		2.7	2.51	0.0058	1 *f*	2.25	0.0072	10.6
		2.2	**2.52**	0.0052	2 *f*	**2.30**	0.0098	10.6 (*)
I1	541	3.5	2.50	0.0067				12.1
		2.9	2.50	0.0055	1 *f*	2.25	0.0123	11.1
		2 *f*	**2.52**	0.0041	2 *f*	**2.31**	0.0074	11.6 (*)
J1	566	3.5	2.50	0.0063				10.4
		3.3	2.50	0.0059	1 *f*	2.28	0.0294	10.4
		2.5 *f*	**2.52**	0.0046	1.5 *f*	**2.32**	0.0083	10.6 (*)
K1	582	3.7	2.51	0.0061				10.3
		3.2	**2.51**	0.0052	1 *f*	**2.28**	0.0145	9.6 (*)
		2.5 *f*	2.52	0.0040	1.5 *f*	2.31	0.0069	10.0
L1	602	4.1	2.53	0.0061				9.0
		3.7	2.53	0.0055	1 *f*	2.29	0.0190	8.7
		3 *f*	**2.53**	0.0041	1 *f*	**2.30**	0.0046	9.4 (*)
H2	510	3.0	2.48	0.0064				13.7
		2.2	2.49	0.0044	1 *f*	2.24	0.0069	12.2
		1.8	**2.50**	0.0038	2 *f*	**2.30**	0.0090	11.9 (*)
I2	519	3.0	2.49	0.0057				13.7
		2.3	2.50	0.0040	1 *f*	2.24	0.0078	11.9
		2.1	**2.50**	0.0039	2 *f*	**2.30**	0.0137	12.0 (*)
J2	547	3.3	2.50	0.0060				9.6
		2.1	2.52	0.0030	1 *f*	2.27	0.0019	8.2
		2 *f*	**2.52**	0.0037	2 *f*	**2.32**	0.0078	8.5 (*)
K2	559	3.2	2.51	0.0056				11.1
		2.5	2.51	0.0042	1 *f*	2.27	0.0087	10.3
		2.5 *f*	**2.51**	0.0043	1.5 *f*	**2.31**	0.0129	10.5 (*)

Solution	^{113}Cd NMR (δ, ppm)	Cd-S			Cd-(N/O)			R^c
		N	*R* (Å)	σ² (Å²)	*N*	*R* (Å)	σ² (Å²)	
L2	575	3.3	2.51	0.0055				9.7
		2.9	2.51	0.0048	1 *f*	2.32	0.0143	9.6
		2.5 *f*	**2.52**	0.0042	1.5 *f*	**2.33**	0.0100	9.8 (*)
M2	578	3.0	2.51	0.0045				8.8
		2.6	2.51	0.0037	1 *f*	2.27	0.0146	8.1
		2.5*f*	**2.52**	0.0036	1.5 *f*	**2.31**	0.0183	8.3 (*)
N2	578	3.4	2.51	0.0061				12.5
		2.5 *f*	**2.53**	0.0048	1.5 *f*	**2.33**	0.0062	11.8 (*)

[a]EXAFS spectra of **M1** and **N1** are not available; (*) fits that are compatible with the observed ^{113}Cd NMR chemical shifts and shown in Figure 4; *f* = fixed; S_0^2 = 0.87 *f*; *N* = coordination number/ frequency; *k*-fitting range = 3.5 - 12.0 Å^{-1};

[b]Residual (%).